



North Pacific Fisheries Commission

NPFC-2020-SSC PS06-WP06

Joint CPUE standardization of the Pacific saury in the Northwest Pacific Ocean during 2001-2019 by using the conventional and geostatistical approaches

Yi-Jay Chang and Jhen Hsu

Institute of Oceanography, National Taiwan University

Abstract

Reliable indices of population abundance are an important type of data for stock assessment. We applied a Vector-Autoregressive Spatio-Temporal Model (VAST) to conduct index standardization by using the joint CPUE (catch-per-unit-effort) data of the Pacific saury in the Northwest Pacific Ocean during 2001 and 2019. The joint CPUE data of stick-held dip net fisheries was collected from each member including Chinese Taipei, China, Japan, Korea, Russia, and Vanuatu in the North Pacific Fisheries Commission (NPFC). Furthermore, we provided a comparison of the CPUE standardization between VAST and the conventional generalized linear model. The objective is to make a suggestion for the appropriate specification of the joint CPUE index to be used in the Pacific saury stock assessment. The results indicated that VAST performs better than the GLM with higher R^2 value, less residuals depart from zero, and smaller residual variance. We recommend using VAST for deriving the standardized joint index as improved input data in the stock assessment. The analysis we presented is generally applicable and should be considered as a standard tool in the CPUE standardization.

1. Introduction

Standardization of commercial catch and effort data is important in fisheries where standardized abundance indices based on the fishery-dependent data are a fundamental input to stock assessments. The nominal CPUE (catch-per-unit-effort) index, derived from yearly means of the raw CPUE data, can be severely biased due to the fishing fleets in specific locales using gear that increases catchability, low fishing effort in areas which give inaccurate average CPUE, oceanography conditions that increase catchability by, for instance, making fish more vulnerable to fishing gear, or simply chance. The most commonly used standardization procedures entail the application of Generalized Linear Models (GLMs) or Generalized Additive Models (GAMs), which aim to isolate temporal abundance trends from the total variation in the CPUE data by adjusting for confounding effects on the estimated abundance trends (Guisan et al., 2002; Maunder and Punt, 2004). In addition, observations that occur closer in space are more likely to be similar (spatial autocorrelation), which makes it harder to distinguish the real signal of a spatial effect by an explanatory variable. Recent years have seen the emergence of

spatiotemporal modelling methods for standardizing CPUE data (e.g., Walter et al., 2014; Thorson et al., 2015; Kai et al., 2017; Grüss et al., 2019), because they allow the spatial autocorrelation to be removed, which may yield more precise, biologically reasonable, and interpretable estimates of abundance than common methods such as GLM (Shelton et al., 2014; Thorson et al. 2015).

Pacific saury (*Cololabis saira*), a migratory small pelagic fish, is widely distributed and migrate over extensive areas of the Northwestern Pacific Ocean. (Fukushima, 1979). This species is commercially important in the Northwestern Pacific Ocean, targeted by stick-held dip net fisheries from several members of the North Pacific Fisheries Commission (NPFC) that the offshore fishing vessels by Japan and Russia operate mainly within the exclusive economic zones while the distant-water vessels of China, Korea, and Chinese Taipei operate mainly east of Hokkaido and the Kuril Islands in the Northwestern Pacific Ocean. In view of the fact that there is a conflict among the standardized CPUE indices derived by members, the 3rd Technical Working Group on the Pacific Saury Stock Assessment (TWG PSSA) aim to develop a single joint CPUE index for the Pacific saury from the catch and effort data by all members (i.e., joint CPUE data).

In this study, we apply a Vector-Autoregressive Spatio-Temporal Model (i.e., VAST, Thorson 2019) to conduct an index standardization by using the joint CPUE data of the Pacific saury in the Northwest Pacific Ocean during 2001 and 2019. Furthermore, we provide a comparison of the CPUE standardization between VAST and the conventional model (i.e., GLM). The objective is to make a suggestion for the appropriate specification of the joint CPUE index to be used in the Pacific saury stock assessment. Progress in joint standardized CPUE should result in better assessment and management of the stock.

2. Methods

2.1 Joint CPUE dataset

The joint CPUE data of stick-held dip net fisheries was collected from each member including Chinese Taipei, China, Japan, Korea, Russia and Vanuatu in the North Pacific Fisheries Commission (NPFC). This dataset was aggregated by year and month with a spatial resolution of $1^\circ \times 1^\circ$ and covered the northwestern Pacific Ocean between $32 - 50^\circ \text{N}$ and $140 - 174^\circ \text{E}$ from 2001 to 2019. Data grooming was applied prior to the standardization to remove the monthly observation with less than 10 operation days. The spatial and temporal pattern of the nominal

CPUE data during 2001 and 2019 was shown in **Figure 1**.

2.2 Conventional CPUE standardization

We use a log offset GLM to standardize CPUE as the following description:

$$\log(C(s_i, t_i)) \sim Yearmonth(t_i) + cell(s_i) + \sum_{j=1}^{n_j} \gamma(j) X(s_i, t_i, j) + \sum_{k=1}^{n_k} \lambda(k) Q(i, k) + \log(Op_day(s_i, t_i))$$

where $C(s_i, t_i)$ is the prediction of Pacific saury catch i (in metric ton) in the $1^\circ \times 1^\circ$ cell s_i and year-month t_i , $Yearmonth(t_i)$ is the fixed effect for each year-month t_i (147 time steps), $cell(s_i)$ is the fixed effect for the $1^\circ \times 1^\circ$ spatial cell s_i (294 cells), $\gamma(j)$ represents the impact of covariate j (i.e., linear impact of SST, $n_j = 1$) with value $X(s_i, t_i, j)$ on catch for cell s_i and year-month t_i . $Q(i, k)$ represent the catchability covariates that explain variation in catchability, $\lambda(k)$ represent the estimated impact of catchability covariates for this linear predictor, and n_k represent the number of catchability covariates. In this study, only the fleet dummy variable was included in the model ($n_k = 1$), and $Op_day(s_i, t_i)$ is the fishing effort (operating day) as a log offset in cell s_i and year-month t_i . The detail information of explanatory variables used in GLM in **Table 1**. The correlation matrix for these explanatory variables of GLM is shown in **Figure 2**.

2.3 Geostatistical CPUE standardization

The approach we used here is adapted from the R package VAST (<https://github.com/James-Thorson-NOAA/VAST>) developed by Thorson et al. (2015). VAST uses the Gaussian random fields to model the spatial autocorrelation with anisotropy (which means the relationship of spatial autocorrelation does not have to change at the same rate in all directions), and an interactive relationship between space and time (i.e., spatio-temporal autocorrelation). These Gaussian random fields are defined with a Matérn covariance function (see Thorson, 2019). VAST requires the previous definition of knots s which are points where the correlation of spatial and spatio-temporal effects are estimated. Each observation in the dataset then gets assigned to the knot which is the closest to them using the k -means. In this study, we specify 100 spatial knots (see **Figure 3** for the configuration) to approximate the spatial and spatio-temporal autocorrelated variations. We confirmed that our results are qualitatively similar when using various numbers of spatial knots (100, 150, and 200 knots) (see **Appendix Figure**

S1).

We give a brief description of how the VAST is applied to the Pacific saury joint CPUE dataset below and refer the readers to the original reference for more technical details (see also Thorson et al., 2019). The logarithm prediction of Pacific saury CPUE, $p(s,t)$, in knot s and year-month t is described below:

$$p(i) = \beta(t_i) + \omega(s_i) + \varepsilon(s_i, t_i) + \sum_{j=1}^{n_j} \gamma(j) X(s_i, t_i, j) + \sum_{k=1}^{n_k} \lambda(k) Q(i, k)$$

where $p(i)$ is the predictor for observation i , $\beta(t_i)$ is the intercept for each year-month t_i as a fixed effect, $\omega(s_i)$ is a time-invariant spatial autocorrelated variation for knot s_i (100 knots), and $\varepsilon(s_i, t_i)$ is a time-varying spatial-temporal autocorrelated variation for knot s_i and in year-month t_i (i.e., the interaction of spatial variation and time). $\gamma(j)$ represents the impact of covariate j (i.e., the linear impact of SST, $n_j = 1$) with value $X(s_i, t_i, j)$ on density for knot s_i and year-month t_i . $Q(i, k)$ are the fixed effects for catchability, $\lambda(k)$ represent the estimated impact of catchability covariates for this linear predictor, and n_k represent the number of catchability covariates. In this study, only the fleet dummy variable was included in the model ($n_k = 1$). The detail information of explanatory variables used in VAST was shown in **Table 2**. The correlation matrix for these explanatory variables of VAST is shown in **Figure 4**.

2.4 Model selection and diagnostics

We used the Akaike Information Criterion (AIC; Akaike, 1973) to identify which model had greater support given available data within the GLM and VAST. Histograms of the residuals were used to assess normality for the GLM and VAST, in addition, the quantile-quantile normal probability plots (Normal Q-Q plot) for both of them. For a better understanding of CPUE standardization of Pacific saury, the “step plots” (Bishop et al., 2008) were conducted to understand the effects of removing individual factors from the GLM and VAST with respect to the estimated CPUE indices.

2.5 Standardized CPUE trends

Predictions of standardized Pacific saury CPUE for observation i then excludes the value for the covariates linked to catchability, here is the fleet but otherwise retains the other predictors of density in space and time. The standardized index for GLM and VAST is respectively described as below:

2.5.1 Conventional CPUE model (GLM)

Estimated values of fixed effects are used to predict the density (defined as catch weight per day) except the catchability variable.

$$C(s,t) = \exp\left(YearMonth(t) + cell(s) + \sum_{j=1}^{n_j} \gamma_j x_j(s,t)\right) \Psi_{C(s,t)}$$

where $\Psi_{C(s,t)}$ is a correction for bias (Bradu and Mundlak, 1970; Lo et al., 1992). Assuming lognormal-distributed errors, the correction factor is:

$$\Psi_{C(s,t)} = g_m \left[\frac{m+1}{2m} (\zeta^2 - \zeta_\eta^2) \right]$$

where g_m is a function described below, ζ^2 is the residual variance, m is degrees of freedom for the estimate of residual variance, $\eta = YearMonth(t) + cell(s) + \sum_{j=1}^{n_j} \gamma_j x_j(s,t)$, and ζ_η^2 is the variance of η . The function g_m is defined as:

$$g_m(t) = \sum_{p=0}^{\infty} \left[\frac{m^p (m+2p)}{m(m+2)\dots(m+2p)} \left(\frac{m}{m+1}\right)^p \frac{t^p}{p!} \right]$$

where t is the argument for the function. Variance estimates for $C(s,t)$ were calculated as:

$$\text{Var}(C(s,t)) = e^{2\eta} \left\{ g_m^2 \left[\frac{m+1}{2m} (\zeta^2 - \zeta_\eta^2) \right] - g_m \left[\frac{m+1}{m} (\zeta^2 - 2\zeta_\eta^2) \right] \right\}$$

Year-month density ($B(t)$) is calculated as the sum of density of each station:

$$B(t) = \sum C(s,t) \times a(s)$$

where $B(t)$ is the area re-weighted density in year-month t throughout the population domain, $a(s)$ is the area of the $1^\circ \times 1^\circ$ spatial cell s (12,100 km²). Annual density is calculated as the averaged density across the month.

2.5.2 Geostatistical CPUE model (VAST)

Estimated values of fixed and random effects are used to predict the density $p(s,t)$ except the catchability variable (Thorson et al., 2019). Year-month density, $B(t)$, is calculated as the sum of density of each station ($p(s,t)$).

$$p(s,t) = \beta(t) + \omega(s) + \varepsilon(s,t) + \sum_{j=1}^{n_j} \gamma(j)X(s,t,j)$$

$$B(t) = \sum \exp(p(s,t)) \times a(s)$$

where $B(t)$ is the area re-weighted density in year-month t throughout the population domain, $a(s)$ is the area of knot s . Furthermore, year-month density was bias-corrected by using the “epsilon bias-correction estimator” (Thorson and Kristensen, 2016) to correct for retransformation bias. Annual density is calculated as the averaged density across the month.

3. Results and discussion

3.1 Model selection and diagnostic

According to the AIC value, we used the most parameterized model (G-4 and V-4) of GLM and VAST to predict the year-month changes in CPUE of Pacific saury, respectively (Tables 3 - 4). The histogram and Q-Q plots of both models based on the lognormal distributions appear normal in GLM and VAST for all fleets (Figs. 5 and 6), which confirms the assumption of the error distribution is generally appropriate for the CPUE standardization. Figure 7 shows that there is no significant residual pattern for each fixed effect in the GLM. For the VAST, a similar result of the residual pattern was found (Fig. 8). The results revealed that the VAST yielded higher R^2 (0.68) than did the GLM (0.32). Generally, the VAST performed better than the GLM with less residuals depart from zero and smaller residual variance.

3.2 Comparison of the standardized indices

Step plots indicated that the *cell* variable has a major influence on standardized CPUE compared to the other effects in GLM (Fig. 9). However, there are incremental changes in the indices when effects were introduced into the VAST successively (Fig. 10). The estimated year-month relative density value from GLM and VAST were shown in Figure 11. Generally, the results of relative density from GLM and VAST showed the same trend across time. However,

the VAST model generated the lower model uncertainty compared to the GLM model. The annual relative density trend indicated there was a fluctuated pattern over studied periods (**Fig. 12**). The relative density was at the lowest level below average (2001-2019) in 2019 in both models. The summary of year-month and annual standardized CPUEs by the GLM and VAST compared with the nominal CPUEs were shown in **Figure 13** and **Table 5**.

Although there is no clear difference in the annual trends of standardized CPUE indices between the GLM and VAST, we recommend using VAST in the future Pacific saury stock assessment according to the better performance in R^2 and the estimated uncertainty in GLM over VAST. Previous study has also suggested that the spatio-temporal modeling platform VAST achieved the best performance among nine CPUE standardization methods by using the simulation testing, namely generally had one of the lowest biases, one of the lowest mean absolute errors, and the probability of the true index been included by the estimated 50% confidence interval is closest to 50% (Grüss et al., 2019). We also recommend using VAST from a practical standpoint that the regional weights, the year-quarter standardized indices, and the corresponding standard errors can be estimated directly as part of the modelling procedure, so no additional step is required to produce them (often not been reported).

References

- Akaike, H. (1974). A new look at the statistical model identification. *IEEE transactions on automatic control*, 19(6), 716-723.
- Bishop, J., Venables, W. N., Dichmont, C. M., and Sterling, D. J. (2008). Standardizing catch rates: is logbook information by itself enough?. *ICES J. Mar. Sci.*, 65(2), 255-266.
- Bradu, D., and Mundlak, Y. (1970). Estimation in lognormal linear models. *J. Am. Stat. Assoc.*, 65(329), 198-211.
- Guisan, A., Edwards Jr., T.C., Hastie, T. (2002). Generalized linear and generalized additive models in studies of species distributions: setting the scene. *Ecol. Mod.* 157, 89–100
- Grüss, A., Walter III, J. F., Babcock, E. A., Forrestal, F. C., Thorson, J. T., Laretta, M. V., and Schirripa, M. J. (2019). Evaluation of the impacts of different treatments of spatio-temporal variation in catch-per-unit-effort standardization models. *Fish Res.*, 213, 75-93.
- Kai, M., Thorson, J. T., Piner, K. R., and Maunder, M. N. (2017). Spatiotemporal variation in size-structured populations using fishery data: an application to shortfin mako (*Isurus oxyrinchus*) in the Pacific Ocean. *Can. J. Fish Aquat. Sci.*, 74(11), 1765-1780.

Lo, N. C. H., Jacobson, L. D., and Squire, J. L. (1992). Indices of relative abundance from fish spotter data based on delta-lognormal models. *Can. J. Fish Aquat. Sci.*, 49(12), 2515-2526.

Maunder, M. N., and Punt, A. E. (2004). Standardizing catch and effort data: a review of recent approaches. *Fish Res.*, 70(2-3):141–159.

NPFC TWG-PSSA. 2018. Report of 3rd Meeting of the Technical Working Group on Pacific Saury Stock Assessment. NPFC-2018-TWG PSSA03-Final Report. 29 pp.

R Development Core Team (2018). R: A language and environment for statistical computing. Vienna, Austria: R Foundation for Statistical Computing. ISBN 3-900051-07-0. Retrieved from <http://www.R-project.org>

Shelton, A. O., Thorson, J. T., Ward, E. J., and Feist, B.E. (2014). Spatial semiparametric models improve estimates of species abundance and distribution. *Can. J. Fish Aquat. Sci.* 71(11): 1655–1666.

Thorson, J. T., Shelton, A. O., Ward, E. J., and Skaug, H. (2015). Geostatistical delta-generalized linear mixed models improve precision for estimated abundance indices for West Coast groundfishes. *ICES J. Mar. Sci.*, 72, 1297–1310.

Thorson, J. T., and Kristensen, K. (2016). Implementing a generic method for bias correction in statistical models using random effects, with spatial and population dynamics examples. *Fish Res.*, 175, 66-74.

Thorson, J. T. (2019). Guidance for decisions using the Vector Autoregressive Spatio-Temporal (VAST) package in stock, ecosystem, habitat and climate assessments. *Fish Res.*, 210:143–161.

Walter, J. F., Hoenig, J. M., and Christman, M. C. (2014). Reducing bias and filling in spatial gaps in fishery-dependent catch-per-unit-effort data by geostatistical prediction, I. Methodology and simulation. *N. Am. J. Fish Manage.*, 34(6), 1095-1107.

Table 1. Summary of explanatory variables used in GLM.

Variables		Number of categories	Detail
Year-month	<i>t</i>	147	$t = 1$ (2001/May) – $t = 147$ (2019/Dec)
Spatial cell	<i>Cell</i>	294	32 – 50 °N and 140 – 174 °E in 1°×1° grid
Sea surface temperature	<i>SST</i>	1	Continues variable (3 -25 °C)
Fleet	Fleet	7	JP1: Japanese vessel less than 100 GRT; JP2: Japanese vessel larger than 100 GRT; CT: Chinese Taipei; CN: China; RS: Russia; KR: Korea; VU: Vanuatu

Table 2. Summary of explanatory variables used in VAST.

Variables		Number of categories	Detail	Note
Year-month	<i>t</i>	147	<i>t</i> = 1 (2001/May) – <i>t</i> = 147 (2019/Dec)	
Spatial knot	<i>s</i>	100	32 – 50 °N and 140 – 174 °E	See Figure 2
Sea surface temperature	<i>SST</i>	1	Continues variable (3 -25 °C)	
Fleet	Fleet	7	JP1: Japanese vessel less than 100 GRT; JP2: Japanese vessel larger than 100 GRT; CT: Chinese Taipei; CN: China; RS: Russia; KR: Korea; VU: Vanuatu	

Table 3. Summary of the model selection information from GLM.

Model No.	Model structure	Number of parameters	Deviance	AIC
G-1	<i>Year-month</i>	147	8146	24329
G-2	<i>Year-month + Cell</i>	440	7341	24015
G-3	<i>Year-month + Cell + SST</i>	441	7334	24009
G-4	<i>Year-month + Cell + SST + Fleet</i>	447	7094	23732

Table 4. Summary of the model selection information from VAST.

Model No.	Model structure	Number of parameters	Deviance	AIC	Maximum gradient
V-1	<i>Year-month</i>	147	35939	71884	< 0.01
V-2	<i>Year-month + Knot+Year-month and Knot</i>	150	35483	71270	< 0.01
V-3	<i>Year-month + Knot+Year-month and Knot+SST</i>	152	35058	70423	< 0.01
V-4	<i>Year-month + Knot + Year-month and Knot + SST + Fleet</i>	159	34934	70206	< 0.01

Table 5. Annual relative (relative to mean) nominal and standardized indices from GLM and VAST for Pacific saury during 2001 and 2019 in the Northwestern Pacific Ocean. CPUE = standardized CPUE, SD = standard error, lower and upper = lower and upper limits of the 95% confidence intervals.

Year	Nominal	GLM					VAST				
		CPUE	SD	Lower	Upper	CV	CPUE	SD	Lower	Upper	CV
2001	0.81	0.69	0.29	0.12	1.25	0.42	0.73	0.23	0.27	1.18	0.32
2002	0.63	0.57	0.24	0.098	1.05	0.42	0.58	0.18	0.24	0.93	0.30
2003	1.08	1.02	0.43	0.18	1.86	0.42	1.11	0.35	0.43	1.79	0.31
2004	1.08	1.12	0.48	0.175	2.08	0.43	1.25	0.41	0.43	2.06	0.33
2005	1.58	1.78	0.74	0.322	3.24	0.42	1.67	0.49	0.70	2.63	0.30
2006	1.31	0.76	0.31	0.158	1.37	0.41	0.70	0.19	0.32	1.08	0.28
2007	1.25	1.08	0.45	0.208	1.96	0.42	1.10	0.33	0.45	1.75	0.30
2008	1.52	1.4	0.57	0.285	2.51	0.41	1.52	0.46	0.62	2.42	0.30
2009	0.89	0.9	0.37	0.167	1.63	0.41	0.82	0.25	0.34	1.31	0.30
2010	0.88	0.85	0.35	0.165	1.53	0.41	0.85	0.26	0.35	1.36	0.30
2011	1.06	1.1	0.45	0.205	1.99	0.41	1.17	0.38	0.43	1.92	0.32
2012	0.92	1	0.43	0.162	1.83	0.43	1.04	0.35	0.35	1.73	0.34
2013	0.98	0.82	0.33	0.167	1.48	0.40	0.87	0.25	0.38	1.36	0.29
2014	1.23	1.39	0.55	0.298	2.47	0.40	1.39	0.38	0.65	2.13	0.27
2015	0.80	1.07	0.45	0.184	1.96	0.42	0.89	0.27	0.35	1.43	0.31
2016	0.75	0.75	0.31	0.15	1.35	0.41	0.75	0.23	0.31	1.19	0.30
2017	0.59	0.78	0.32	0.148	1.42	0.41	0.85	0.29	0.27	1.42	0.35
2018	1.16	1.37	0.57	0.248	2.49	0.42	1.26	0.40	0.47	2.05	0.32
2019	0.47	0.55	0.3	-0.032	1.14	0.55	0.45	0.11	0.23	0.67	0.25

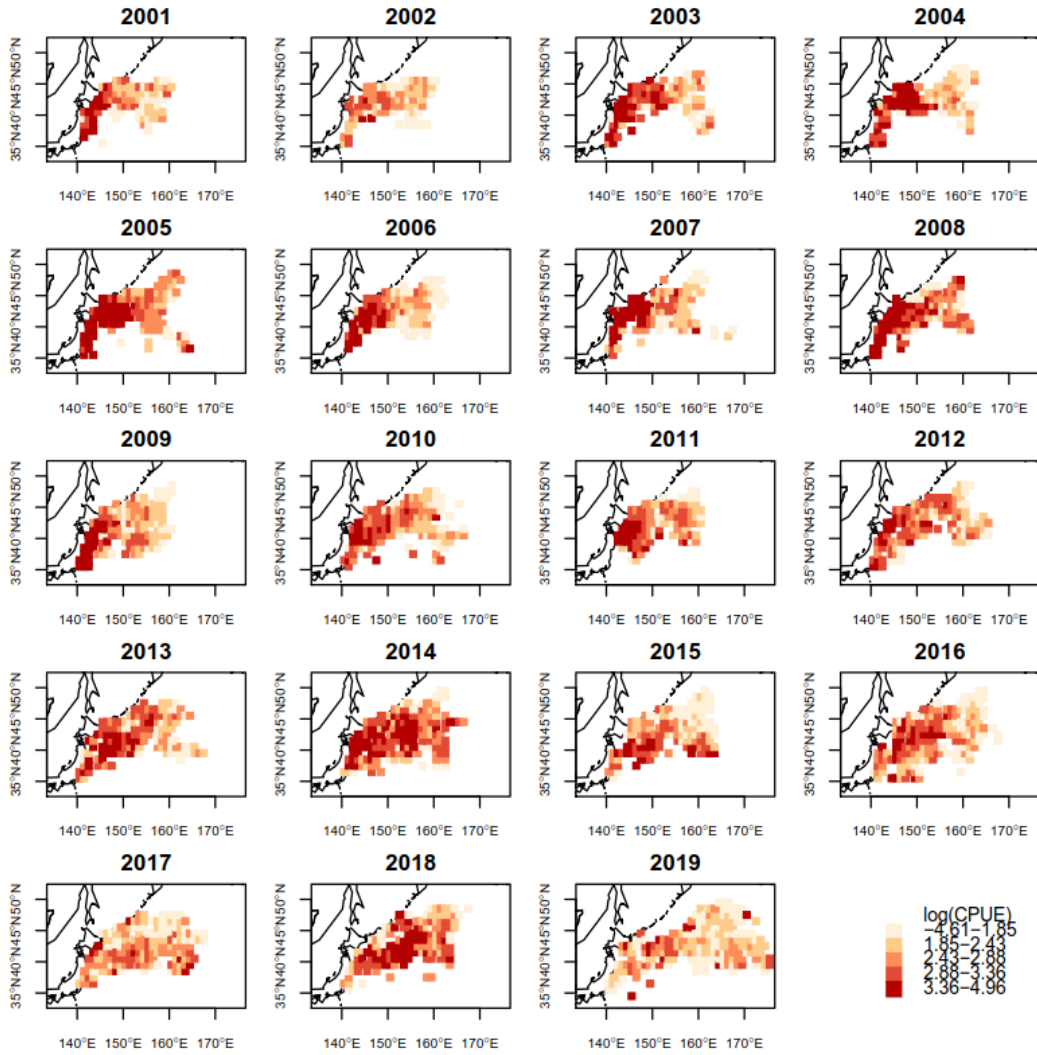


Figure 1. Spatial and temporal distribution of the nominal CPUE (metric ton per operating day fished) of Pacific saury during 2001 and 2019 in the Northwestern Pacific Ocean.

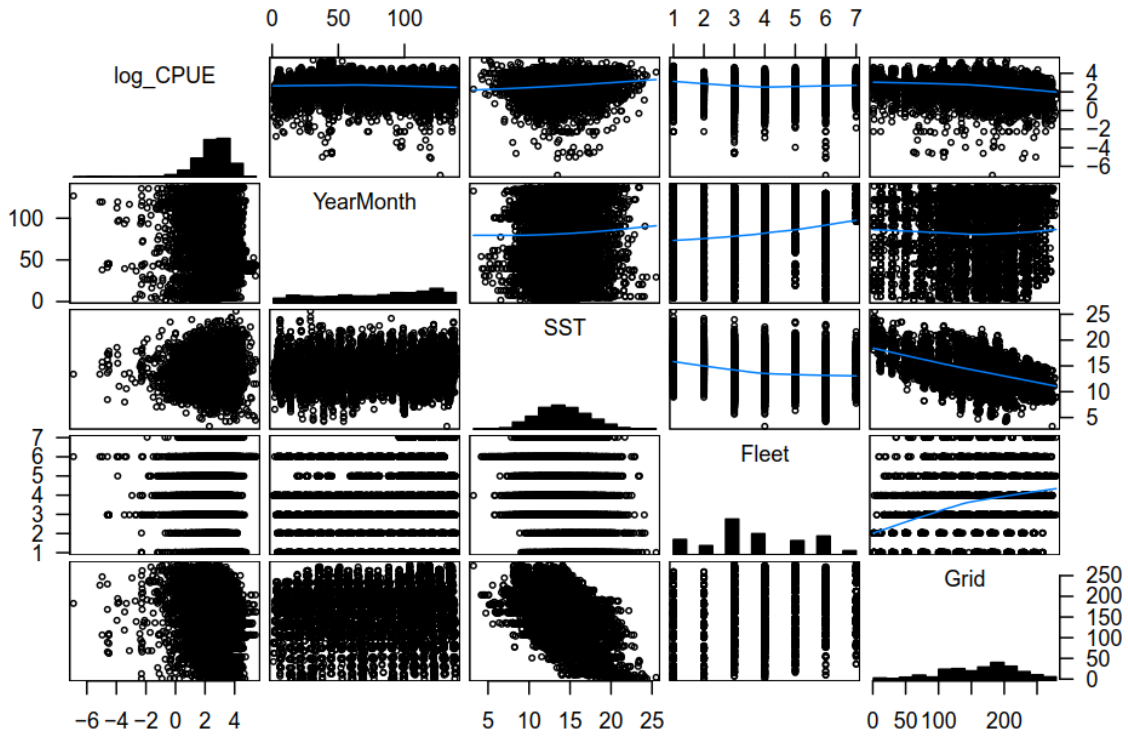


Figure 2. Correlation matrix of explanatory variables used in GLM analysis. The blue curves in the upper triangular matrix denote the loess smooth curves.

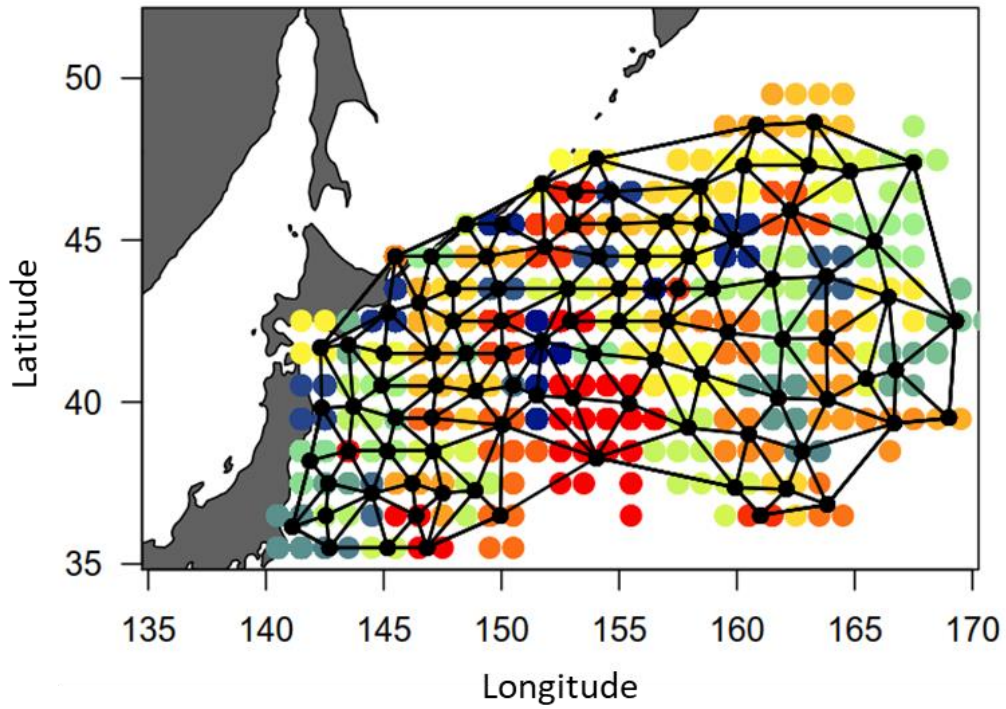


Figure 3. Mesh used to fit the geostatistical model (VAST). An effect is estimated for each of the 100 core knots (black). The colored circles grouped by knots indicate the locations of spatial observations of the Pacific saury from 2001 to 2019 within the $1^\circ \times 1^\circ$ grid.

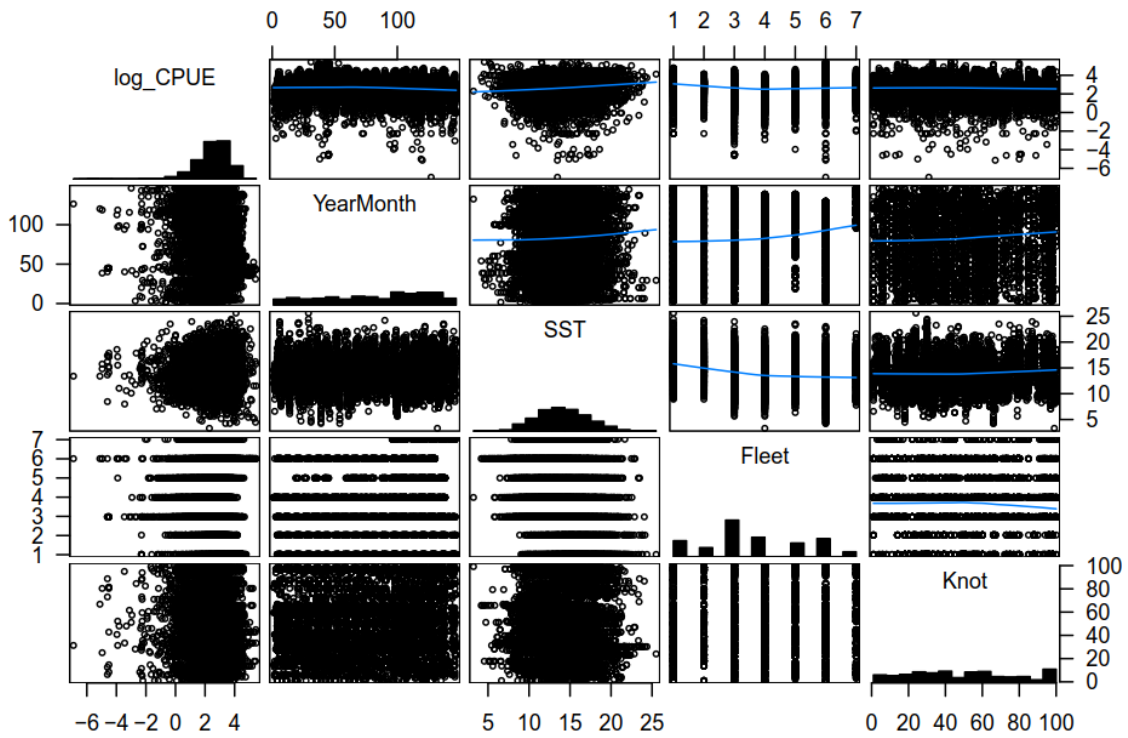


Figure 4. Correlation matrix of explanatory variables used in VAST analysis. The blue curves in the upper triangular matrix denote the loess smooth curves.

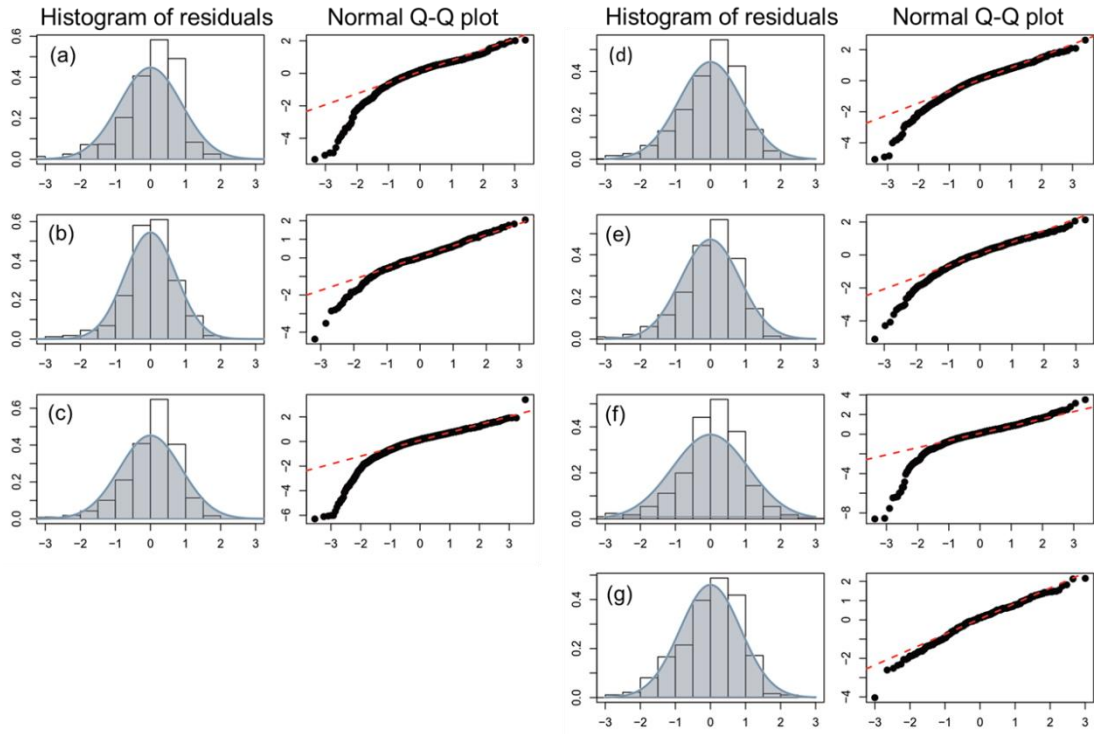


Figure 5. Diagnostic plots of the fitted GLM. The histogram of residuals (left) and Q-Q plot (right) from (a) Japanese fisheries by vessels of <100 ; (b) Japanese fisheries by vessels of ≥ 100 ; (c) Chinese Taipei; (d) Korea; (e) China; (f) Russia, and (g) Vanuatu fisheries.

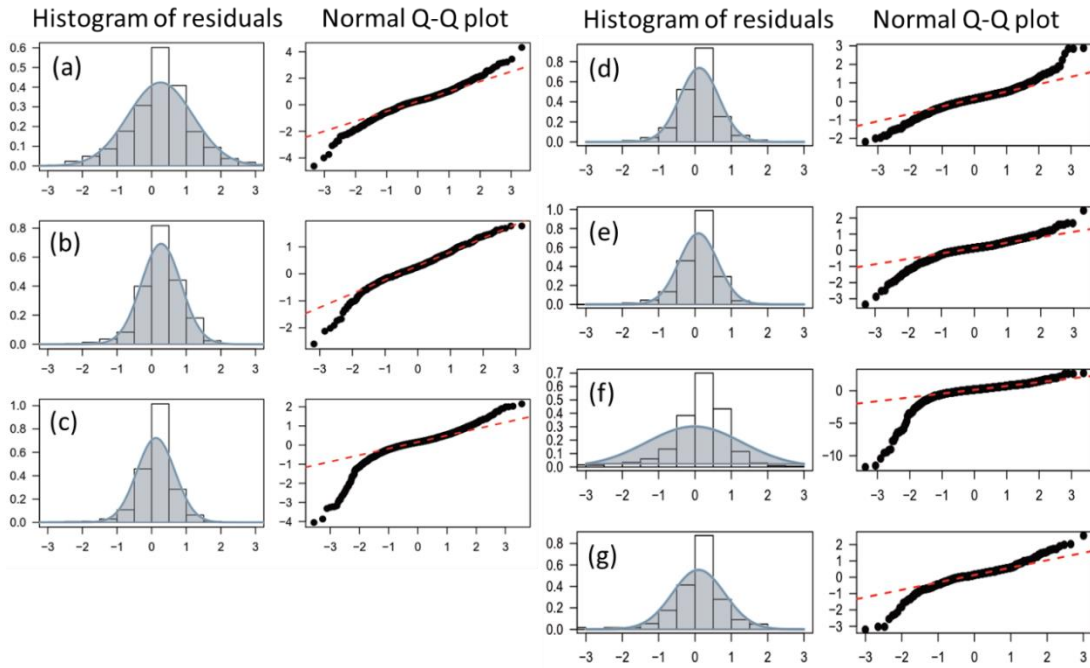


Figure 6. Diagnostic plots of the fitted VAST. The histogram of residuals (left) and Q-Q plot (right) from (a) Japanese fisheries by vessels of <100 ; (b) Japanese fisheries by vessels of ≥ 100 ; (c) Chinese Taipei; (d) Korea; (e) China; (f) Russia, and (g) Vanuatu fisheries.

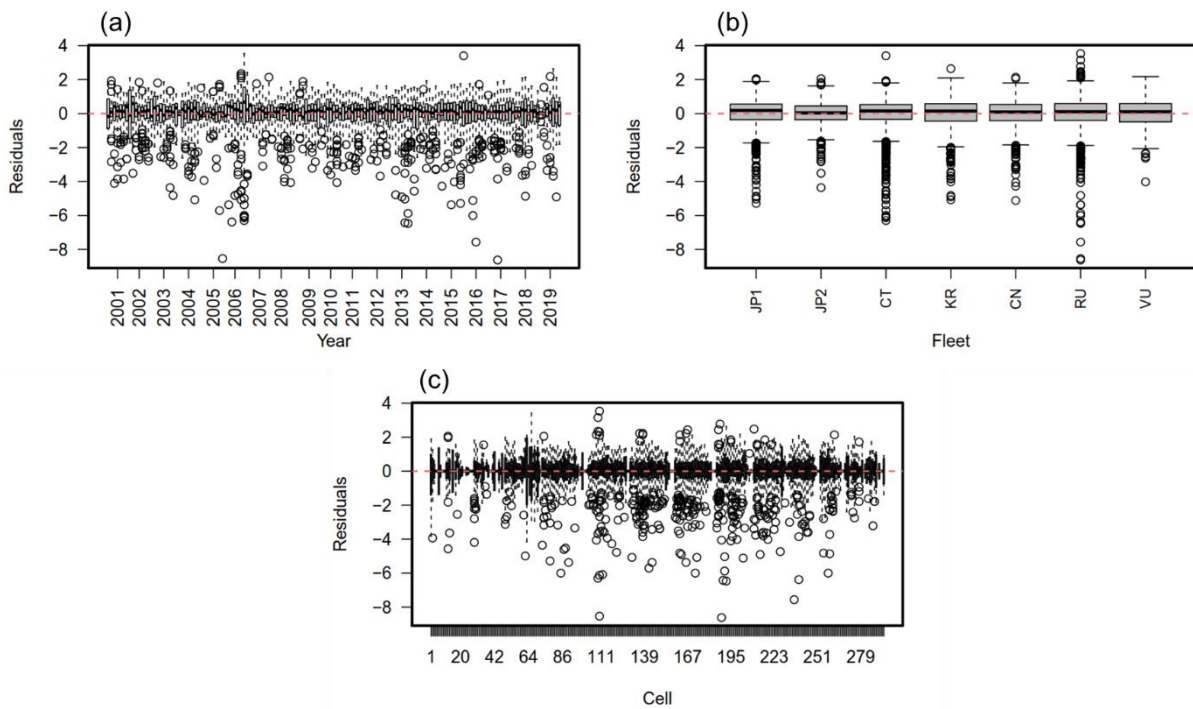


Figure 7. Boxplots of residuals from the GLM by (a) year-month, (b) fleets, and (c) cells of the fitted GLM. JP1 is Japanese fisheries by vessels of <100 ; JP2 is Japanese fisheries by vessels of ≥ 100 ; CT is Chinese Taipei; KR is Korea; CN is China; RU is Russia, and VU is Vanuatu.

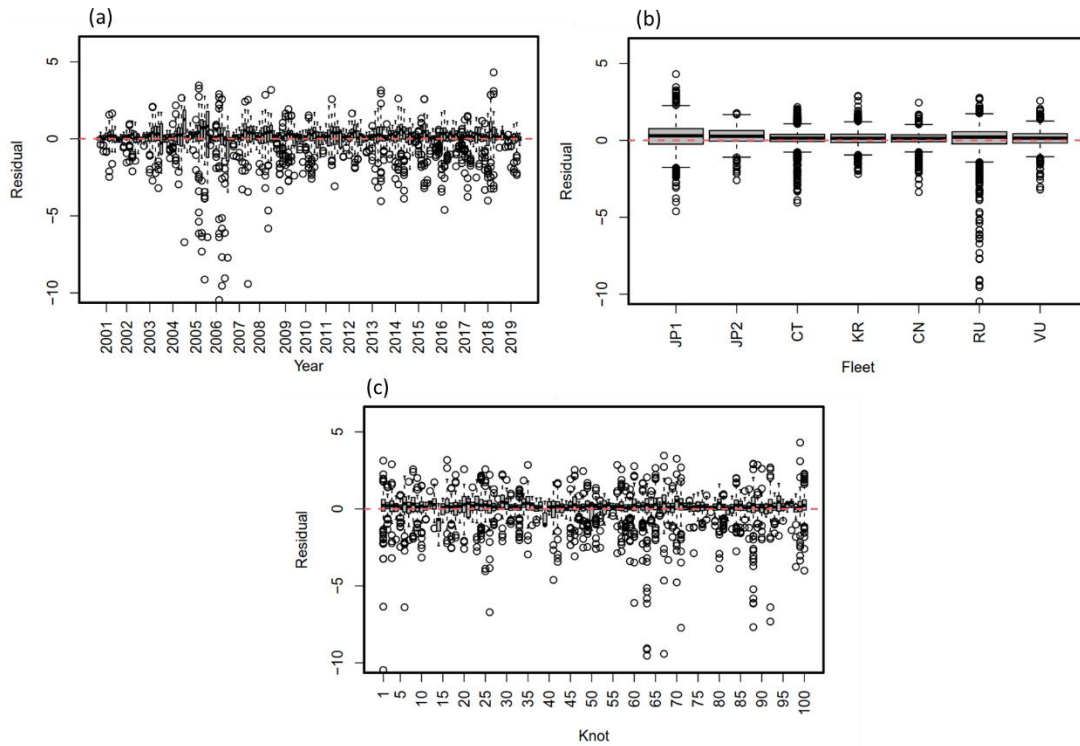


Figure 8. Boxplots of residuals from the VAST by (a) year-month, (b) fleets, and (c) cells of the fitted GLM. JP1 is Japanese fisheries by vessels of <100 ; JP2 is Japanese fisheries by vessels of ≥ 100 ; CT is Chinese Taipei; KR is Korea; CN is China; RU is Russia, and VU is Vanuatu.

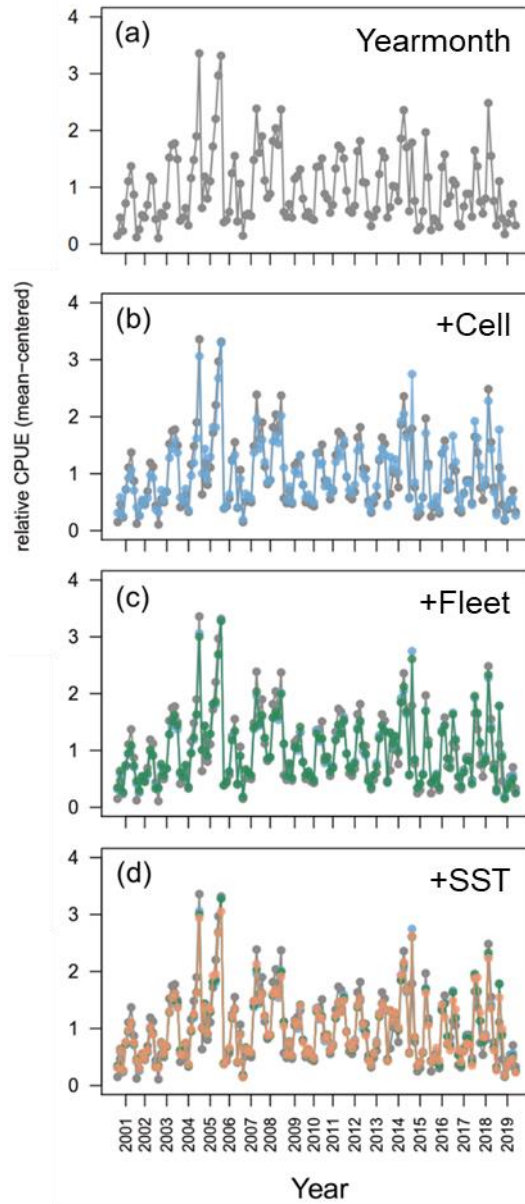


Figure 9. Step plots showing the effects of removing individual factors from the GLM with respect to the estimated CPUE indices.

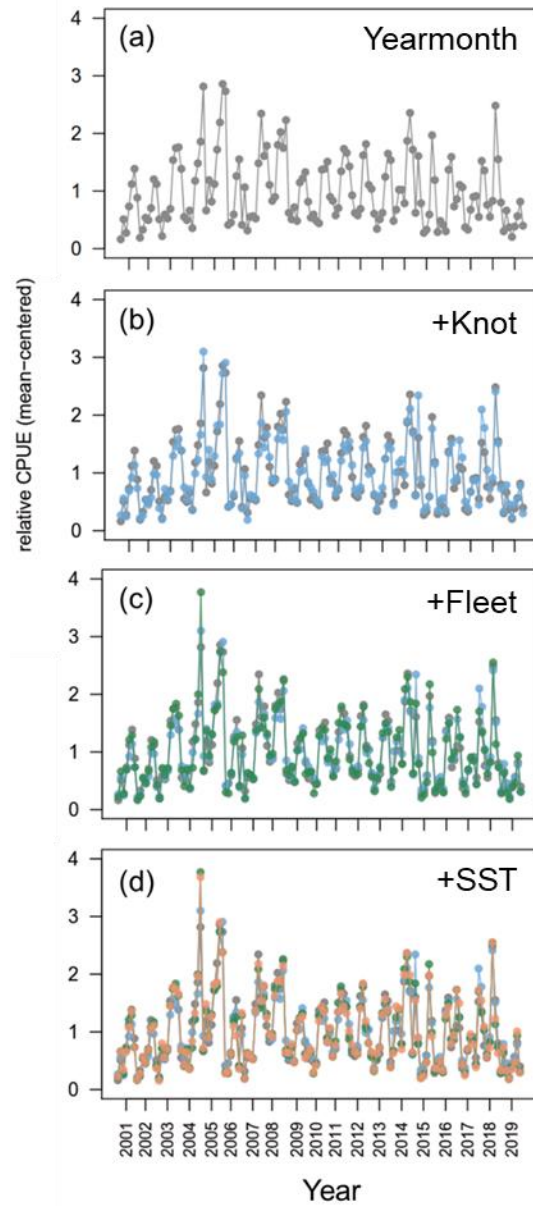


Figure 10. Step plots showing the effects of removing individual factors from the VAST with respect to the estimated CPUE indices.

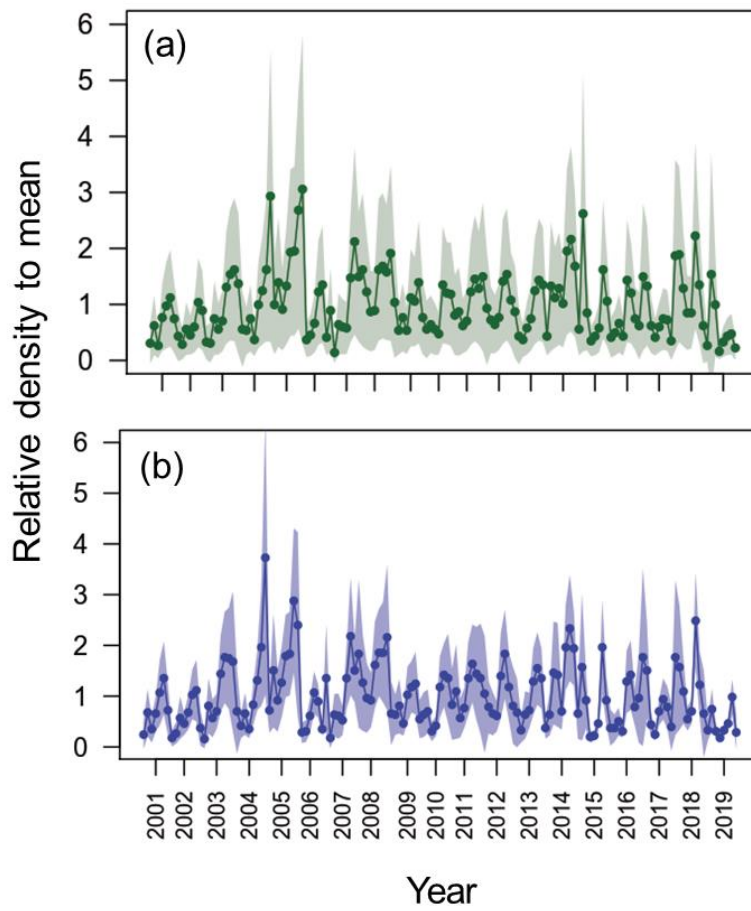


Figure 11. Time-series of year-month relative standardized indices (relative to mean) from the GLM (a) and VAST (b) for the Pacific saury in Northwest Pacific Ocean from 2001 to 2019. The shaded areas denote the 95% confidence intervals.

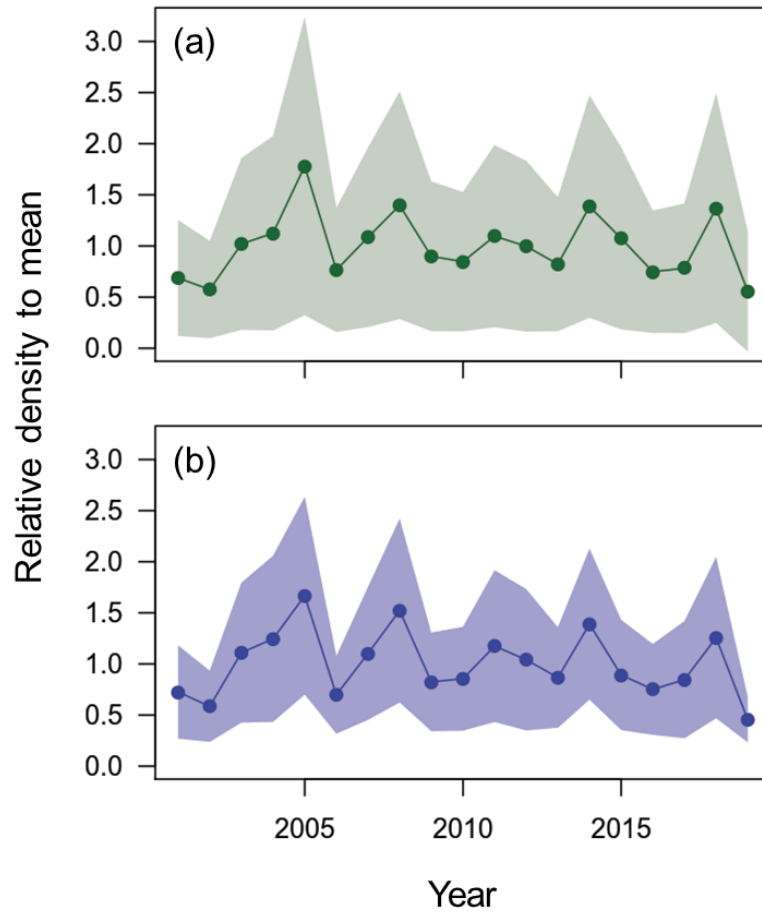


Figure 12. Time-series of annual relative standardized indices (relative to mean) from the GLM (a) and VAST (b) for the Pacific saury in Northwest Pacific Ocean from 2001 to 2019. The shaded areas denote the 95% confidence intervals.

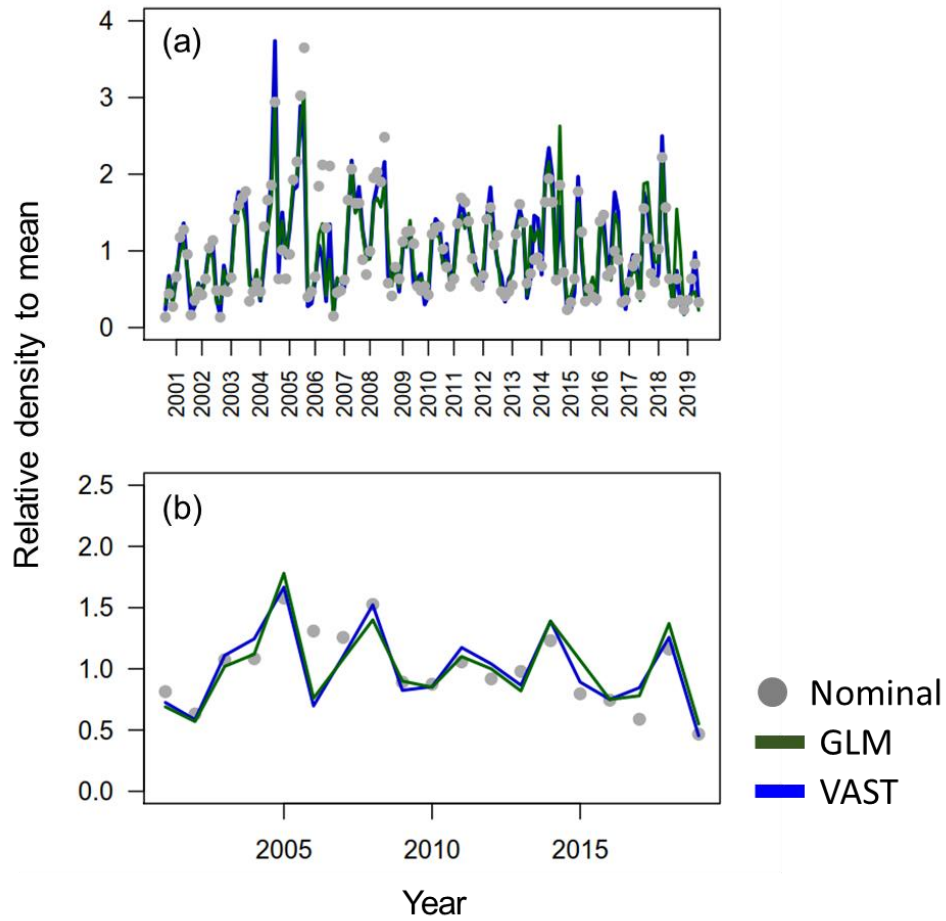


Figure 13. Time-series of year-month (a) and annual (b) relative standardized indices (relative to mean) from the GLM and VAST overlapped with the nominal CPUE (metric ton per operating day fished) for the Pacific saury in Northwest Pacific Ocean from 2001 to 2019.

Appendix S1.

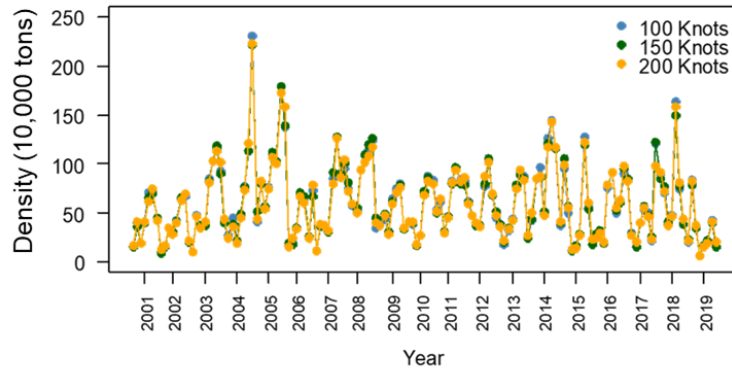


Figure S1. Comparisons of time-series of year-month standardized indices by using various numbers of spatial knots ($n = 100, 150,$ and 200) in the VAST for the Pacific saury in Northwest Pacific Ocean from 2001 to 2019.